

Article

Si-N Matrix as an Effective Fire Retardant Source for Cotton Fabric, Prepared through Sol–Gel Process

Zeeshan Ur Rehman *, Laila Khan, Lee Hwain, Yun Chiho and Bon Heun Koo * 

College of Mechatronic Engineering, Changwon National University, Changwon 51140, Republic of Korea; coatxp@gmail.com (L.K.); 20145130@changwon.ac.kr (L.H.); yunch0430@gs.cwnu.ac.kr (Y.C.)

* Correspondence: zeeshan.physics@gmail.com (Z.U.R.); bhkoo@changwon.ac.kr (B.H.K.)

Abstract: In this study, process control factors such as dipping time, heat treatment time and curing conditions were optimized to prepare N-Si network sol–gel-based coatings on a cotton fabric. The dipping time was varied from 14 h to 30 min, the heat treatment time at ~90 °C was varied between no heating conditions to 15 h and the curing was performed at 165 °C. The microstructure of the coating was analyzed using low electron scanning microscopy (LV-SEM), while a compositional study of the coated substrate was carried out using FTIR and EDS techniques. From the thermal and combustion analysis of the coated samples using thermogravimetric and vertical flame test techniques, significant resistance to the degradation process was observed, particularly in the initial stages, in addition to the highest char residue for DI-0.5 h-15~32.93%. Similarly, for DI-5 h-RT, the peak degradation temperature was around ~372 °C, accompanied by a notable char residue of approximately 31.12%. The flame spread and burning rate profile further supported the findings; DI-0.5 h-15 and DI-5 h-RT had the lowest flame spread.

Keywords: Si-N; sol–gel; combustion; fire retardant; thermal properties; FTIR; UL-94; TGA



Citation: Rehman, Z.U.; Khan, L.; Hwain, L.; Chiho, Y.; Koo, B.H. Si-N Matrix as an Effective Fire Retardant Source for Cotton Fabric, Prepared through Sol–Gel Process. *Fire* **2024**, *7*, 69. <https://doi.org/10.3390/fire7030069>

Academic Editors: Yan Ding, Keqing Zhou and Kaili Gong

Received: 14 December 2023

Revised: 14 February 2024

Accepted: 19 February 2024

Published: 26 February 2024



Copyright: © 2024 by the authors. Licensee MDPI, Basel, Switzerland. This article is an open access article distributed under the terms and conditions of the Creative Commons Attribution (CC BY) license (<https://creativecommons.org/licenses/by/4.0/>).

1. Introduction

Cotton is the most widely used natural fiber due to its softness, breathability, safety, affordability, regeneration ability, strength, elasticity, biodegradability and hydrophilicity [1,2]. Cotton is a well-known naturally available bio-source, which can be utilized in wide-scale industrial applications ranging from textiles to high-tech electronics and the medical, nanotechnology and communication industries [3–6]. However, all these potential applications are hindered due to several major drawbacks of the cotton fabric, such as low limiting oxygen index (LOI~18%), high peak heat release rate (PHRR~200–270 w/g) and heat release capacity (HRC~10.6), no self-extinguishing behavior and lower combustion temperature/self-ignition temperature (360–425 °C), which makes it highly flammable; thus, these pose challenges in many high tech and local applications [7–10].

Consequently, cost-effective, user friendly and eco-friendly ways and techniques must be found to produce coatings on cotton fabric in order to cope with the stated thermal vulnerability of the cotton fabric. Various ways were applied to modify the surface of the cotton for enhanced fire retardance, such as ultrasonic radiation [11,12], thiol-ene click chemistry, plasma-induced grafting, photo-induced grafting, layer-by-layer (LBL) and organic and inorganic sol–gel processes [13–29].

In general, the sol–gel process is extremely practical for attaching inorganic and organic thin films to textiles because of their uneven surface topography and ability to withstand harsh environments. Under mild circumstances, the numerous hydroxyl functionalities present on the cellulosic substrate can be effectively employed to covalently attach the sol–gel coatings to the textiles (inorganic/organic hybrid thin films), thereby enhancing their resilience to frequent washing treatments, which are a common occurrence for textiles [30–33]. Therefore, it has been used as an economical and environmentally safe

method of constructing heat- and fire-resistant coatings to increase the flame retardancy of textiles [22,34]. Furthermore, its industrial use can be implemented using the existing technology of industrial surface finishing systems.

The effectiveness of a traditional sol–gel coating made from metal-alkoxide and alkoxy silane precursors in decreasing the flammability of natural and synthetic fibers is often quite low. Thus, to further increase the flame-retardant efficacy of the hybrid materials, sol–gel systems modified with halogen-, phosphorus- and/or nitrogen-rich compounds as synergists have been produced [35–38]. Using these various kinds of materials, and the sol–gel technique, fire retardance of the substrate material can be achieved through either the condensed phase mechanism or gaseous phase mechanism. However, the inclusion of these chemicals in the deposited coating systems could produce unwanted hazards and toxic chemicals, which are under serious restrictions from environmental and health organizations.

For instance, various efforts have been conducted to pursue sol–gel-based coating techniques for various vulnerable substrates such as cotton fabric, polyester fabric, nanocomposite fibers, blended textile fabrics, etc. [3,39–45]. However, there are certain consistent issues with these coatings that the scientific community are still facing. The foremost issue is that the chemicals used are hazardous and expensive. At the same time, due to the evolution of new methods, less interest has been granted to the sol–gel technique through the years, even though it is the simplest and most effective way of depositing coatings on a variety of substrates if optimized effectively. Therefore, the search for new, efficient and relatively environmentally benign chemicals for the sol–gel system to impart fire retardance has always been a hot topic of research for researchers and scientists. This study worked to use simple and relatively non-toxic and non-hazardous chemicals for fire retardant coatings. The study was performed using an acidic precursor and N-based additives for depositing highly flame retardant coatings on cotton.

2. Experiment and Analysis

2.1. Materials and Methods

The cotton fabric (100%) used in this experiment as a substrate material was purchased from the local market. The cotton samples were cut into equal pieces before the experiment (height/width~230 mm/120 mm), and each piece was cleaned and dried in preparation for the experiment. Ethanol and hydrochloric acid were brought from Samchun Korea Industry (Pyeongtaek-si, Republic of Korea). Tetraethoxysilane (TEOS) and melamine were acquired from Sigma Aldrich (St. Louis, MO, USA). In the experiment, 18.6 Ω -cm of DI water was utilized.

2.2. Sol–Gel Matrix Preparation

Before starting the coating, the sol solution was first prepared using the chemicals TEOS:ETHANOL:DI with a ratio of 1:2:4. These chemicals were then mixed into a beaker, and 10 mL of HCl (37%) was added; then, they were stirred at room temperature for 4 h. After that, a clear transparent sol was formed.

A melamine solution ~10% was prepared using DI water and was mixed into a sol solution. The whole solution was stirred again at room temperature for 4 h. The solution was then poured into a new beaker for cotton impregnation.

2.3. Coating Deposition Process

To deposit sol–gel coatings on the cotton fabric sample, a total of 8 samples were used in order to carry out the deposition process under various conditions. The cotton samples with dimensions of (230 mm \times 120 mm) were numbered and deposited under various conditions, as follows: #1 and 2 were used as control cotton fabric. #3,4, named (DI-0.5 h-15), were treated for 0.5 h, dried for 15 h at 90 $^{\circ}$ C and cured at 165 $^{\circ}$ C for 1 min. #5,6, named (DI-2 h-15), were treated for 2 h, dried for 15 h at 90 $^{\circ}$ C and cured at 165 $^{\circ}$ C for 1 min. #7 and 8, named (DI-14 h-5), were treated for 14 h, dried for 5 h at 90 $^{\circ}$ C and cured at 165 $^{\circ}$ C

for 1 min. #9, 10, named (DI-5 h-RT), were treated for 5 h, dried at room temperature and curing was performed for 1.0 min at 165 °C. Table 1 displays all of the parameters in a detailed format.

Table 1. Process control parameters.

Samples	Dipping Time (h)	Heat Treatment 90 °C, Time (h)	Curing, 165 °C, Time (min)
DI-0.5 h-15	0.5	15	1 min
DI-2 h-15	2	15	1 min
DI-14 h-5	14	5	1 min
DI-5 h-RT	5	0	1 min

2.4. Characterization and Measurement Techniques

Low voltage scanning electron microscope (LV-SEM) was used to observe the surface morphologies, texture and uniformity of the deposited coatings. The connected EDX (energy-dispersive X-Ray spectroscopy) tech was used to examine the elemental composition of the coating surfaces (vide infra). To carry out the surface analysis, the coated samples were Pt-sputtered for 3 min in order to have effective electron conduction on the cotton surface. ATR-FTIR (attenuated total reflection–Fourier transform infrared) spectra (JASCO 6300) in the 4000–400 cm^{-1} frequency range were then used to evaluate the samples. Following 32 scans at a resolution of 4 cm^{-1} , the spectra profiles were recorded. Subsequently, using the Scinco Thermogravimetric Analyzer (N-1000/1500) in the temperature range of 25 to 700 °C (Heating rate of 20 °C min^{-1}), the coated and uncoated cotton fabric samples were examined for thermal stability in the presence of nitrogen atmosphere (20 mL/min). The mass of each sample used for TGA was ~10–15 mg. A macro-combustion investigation such as the VFT (vertical flame test) was carried out for all the coated and uncoated samples according to established ASTM D6413 guidelines. Accordingly, a flame was introduced using a Bunsen burner flame source and a lab-made vertical flammability box (300 mm/120 mm). The flame was applied for 10 s and held at an angle of 45° and 20 mm below the fabric sample. The process was recorded using a high-speed optical camera.

3. Results and Discussion

3.1. Coatings Microstructure and Composition

General images of the uncoated and coated samples, obtained under various conditions, can be seen in Figure 1a–e. It can be observed that for longer heating times, the color of the samples changed, in addition to severe self rupturing caused by the stress and tension imparted to the cotton fabric upon coating deposition. Furthermore, mechanical disintegration of the coated samples occurred, as shown in DI-0.5 h-15, DI-2 h-15 and DI-14 h-15, while the other samples resisted mechanical distengraton. The colour change and excessive rupturing suggest partial degrdation of the caoted samples, however this varied with dipping time and heating conditions. The complex network of acid–silica might result from the heating process, which could have possibly augmented the pre-exothermic reactions in the highly flammable environment and thus damaged the molecular structure of the cotton fabric for the samples coated with longer dipping times. In contrast, less physical appearance and breaking of the cotton fabric were observed, caused by the decrease in the level of exothermic reactions with no heating process. Contrary to the heat-treated samples, as the heating time reduced to “0” hours, the cotton fabric could be seen as resistant to self-rupturing and color changes. To further investigate and understand the microstructural features of the coatings, low-voltage scanning electron microscopy was used to inspect the surface topography and microstructure, as shown in Figure 2a–d. The cotton fabric is cellulosic in nature, containing oxygen and carbon molecules, and thus, to avoid the risk of damaging these molecular networks, low-voltage SEM was used. Further, the LV-SEM could reveal the micro-structural details of the coating matrix at the individual

fabric level. Thus, from the SEM images, the rupturing of the individual fabric can be observed at the individual fabric level, in agreement with the macro images. It can be seen that deposition of the coating samples increased with an increase in the dipping time, as shown in Figure 2a–d. Samples coated for 30 min (0.5 h) had the lowest quality of coating (thinner coating); however, as the dipping time increased, the level of the attached coating increased, particularly for the 14 h dipping time. Localized substrate zones, as indicated by the arrow in the figure, can be seen as covered by the coating samples. However, as the dipping time further decreased, the attached coating decreased, and thus a uniform coverage of the whole fabric can be achieved. It is believed that as the time passes (increase in dipping times), the sol–gel matrix becomes more saturate and thus the affinity of the coating to attach with the cotton fabric increases. In addition, the saturation of the sol–gel matrix causes localized coverage of the cotton fabric. Chunks of the coating matrix can be seen in sample DI-14 h-5. Cracks and broken parts, as can be seen on the coated surface of the fibers, suggest a brittle and unstable composition of the coating. This might have occurred due to the irregular deposition and high acidic level, where various fibers zones can also be seen as split apart, particularly in the case of samples # DI-0.5 h-15 and DI-2 h-15. It is important to note that the deposition layers could not alter or conceal the originality and compact nature of the cotton fabric, and thus, the original weave structure of the cotton fabric can be seen.

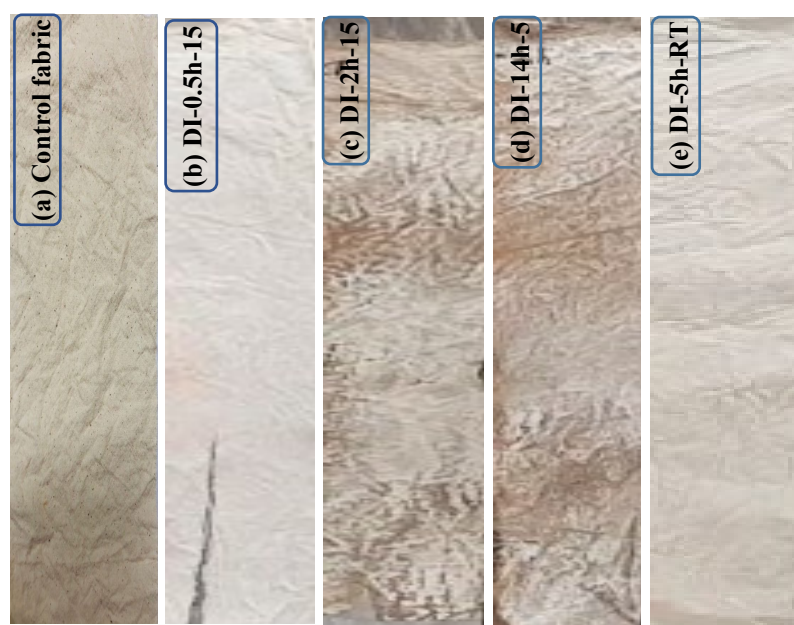


Figure 1. Optical images of coated samples showing color range and other physical properties (a) Control fabric (b) DI-0.5 h-15, (c) DI-2 h-15, (d) DI-14 h-5 and (e) DI-5 h-RT.

The elemental composition of the coating was inspected using EDS analysis techniques, conjointly attached with the SEM microscopic equipment. An elemental profile for each coating can be seen in Figure 3a, supported by the quantitative outline, as in Table 2. The major components of the precursors can be seen as “C” Si, Cl, N and O. From the ethanol and cotton fabric, C and O were obtained, whereas Si was obtained from TEOS. “Cl” was obtained from HCl, whereas “N” was deposited in a lesser amount compared to other components, as can be seen in Table 2 and the elemental profile plot. The presence of an excessive amount of “Si” suggests successful deposition of the sol–gel components to the individual fibers and could help to protect the coated fabric against fire. The percentage of the “Si” can be seen as a monotonic relationship with dipping time, as can be seen from the quantitative values. Initially, for 0.5 h, Si ~7.89% was obtained. However, as the dipping time increased, the percentage of the “Si” increases. With recurring decrease in the dipping time, “Si” followed suit and 11.40 % was obtained. The peak intensities were found to

be random with the non-uniform coatings obtained in the different samples. However, a contrasting trend can be observed for “N”. “N” was higher with lower dipping times, at $\sim 12.37\%$. However, it decreased with increasing dipping times and finally reached $\sim 7.35\%$. As the dipping time decreased again, the percentage of “N” again rose.

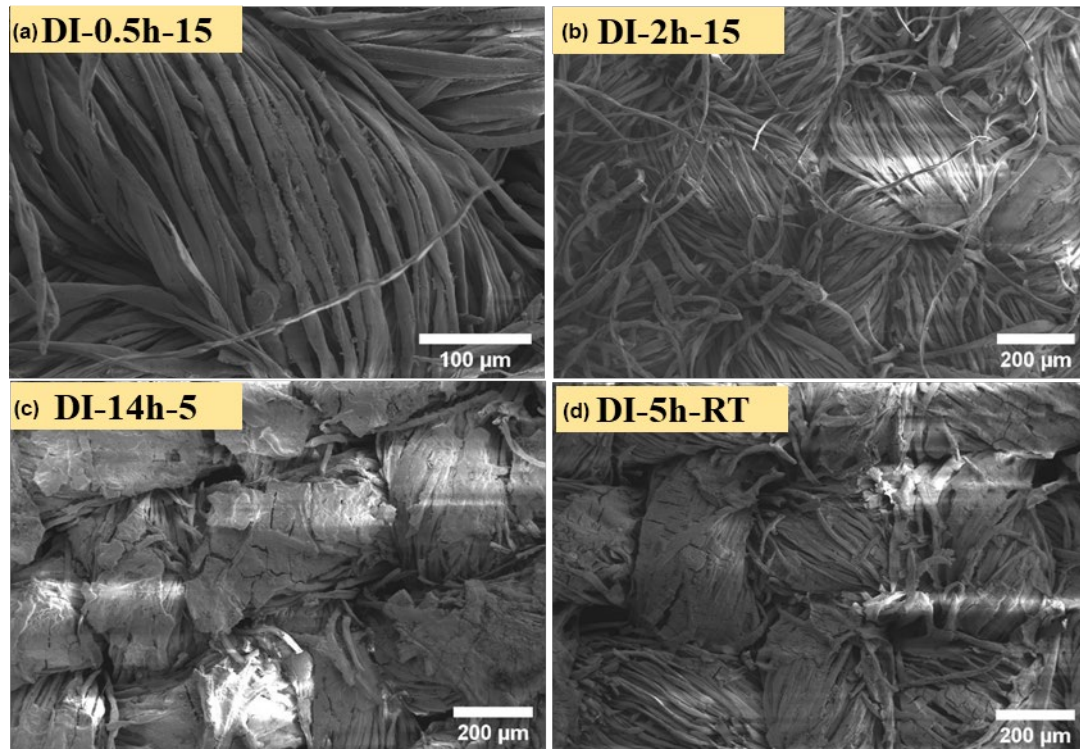


Figure 2. LV-SEM surface micrograph of the coating deposited on the cotton fabric (a) DI-0.5 h-15, (b) DI-2 h-15, (c) DI-14 h-5 and (d) DI-5 h-RT.

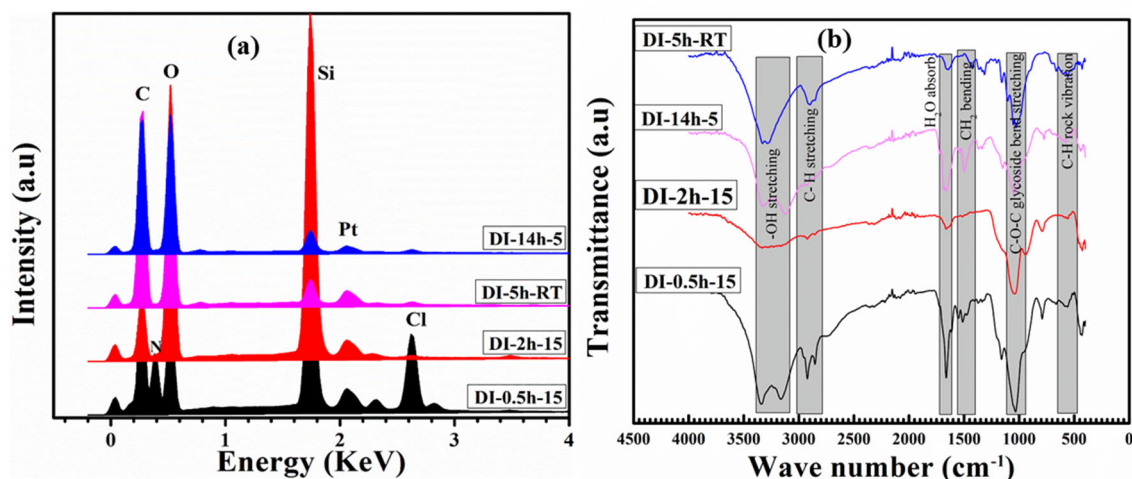


Figure 3. (a) EDS profiles and (b) ATR-FTIR spectra of the coated samples.

Figure 3b shows FT-IR spectra of the coated and uncoated samples, which were used to explore the molecular composition of the coated samples and verify the successful deposition of coatings onto cotton fabrics from the obtained absorption bands. The peaks obtained in the recorded spectra can be ascribed to various stretching and vibrational modes of the bonds between the coating and substrate samples. The following major stretching and vibrational modes were recorded as C–O–C glycoside bend stretching, C–H rock vibration, hydroxyl group “–OH” stretching, –CH stretching, H₂O absorption, –CH

absorption and CH₂ bending. From the FTIR profile, the bands around ~2900 cm⁻¹ can be associated with –CH and CH₂. It can be seen that increased dipping time causes a blue shift in the OH peak position, suggesting a reaction between the cellulosic units and “H” from the acidic samples. Furthermore, with longer dipping times, the peak intensity and split of the OH band becomes more noticeable, as shown in Figure 3b. OH and CH stretching can be seen at higher wave numbers, ~2500 cm⁻¹, signifying lower energy values for these vibrational modes. It is believed that the C–H and O–H functional groups present in the ethanol and cotton fabric could be the primary sources for CH and OH vibrations. Furthermore, it is evident that the coating conditions have a considerable impact on the width of these two peaks, suggesting removal of the OH groups with longer heating processes. The C–H stretching caused by the “H” from the acidic samples decreases with increased dipping times, suggesting an increased quantity of “Si” replacing the “H” samples. Therefore, the C–H absorption peaks can be seen as intensive in the case of the 0.5 hr and 5 h times; however, they weaken with 14 hr dipping. It is noteworthy that the stretching of the Si–O–cellulose and Si–O–Si– linkages is responsible for the peak shift and modification seen at 1200 and 1135 cm⁻¹, indicating the effective deposition of the coating layers. It is important to note that the peaks and peak-lets obtained at 1480 cm⁻¹ and 1040 cm⁻¹ are ascribed to the Si–N peaks, further strengthening the argument of systematic deposition of the sol–gel components to cotton fabric. Further, C=N benzimidazole rings alongside the CH₂ group were also observed as can be seen in the FTIR plot [46].

Table 2. EDS profile values of the coated samples.

# (wt%)	DI-0.5 h-15	DI-2 h-15	DI-14 h-5	DI-5 h-RT
C	34.22	31.57	50.65	52.07
N	12.37	8.10	7.35	8.54
O	24.68	49.73	46.69	46.29
Si	7.89	18.54	2.08	1.40
Cl	4.84	0.16	0.44	0.24
Total:	100.00	100.00	100	100

3.2. Thermal and Combustion Analysis

The thermal degradation process of the control and treated samples in a nitrogen and air atmosphere was investigated using thermogravimetric analysis, and the characteristic curves of the respective TGA and DTGA can be seen in Figures 4 and 5. A lot of information can be obtained from the TGA and DTGA curves, such as T_{5%} (temperature at which mass loss ~5%), which is regarded as the temperature of starting degradation, and T_{max}, which is the maximum rate of degradation and char residual quantity at ~700 °C, as listed in Table 3. The highest T_{on} (which is the starting point of combustion) was obtained for DI-5 h-RT of ~314.09 °C with a respective T_{off} (ending point of combustion) of ~366.59 °C. In contrast, the lowest T_{on} was obtained for the sample DI-2 h-15, of ~296.53 °C, and the T_{off} was ~357.90 °C. The difference in the T_{on} suggests that degradation of DI-2 h-15 was initiated 20 °C earlier than that of DI-5 h-RT. The char residue of the coated samples obtained at 700 °C was ~32.93%, ~28.50%, ~17.86% and ~31.12% for DI-0.5 h-15, DI-2 h-15, DI-14 h-5 and DI-5 h-RT, respectively. It can be observed that the higher residue obtained for DI-0.5 h-15 and DI-5 h-RT was either due to the lower dipping time or lack of heat treatment. The higher dipping time caused the acidic samples to affect the cotton fabric and thus could easily degrade during thermal degradation. Likewise, a longer dipping time and slight heat treatment could aggravate the degradative effect of the acid samples in the coating matrix. The superior anti-degradative behavior of DI-5h-RT can be attributed to the complex network of the N-Si-Cellulose formed at optimum conditions of 5 h dipping and no heating, thus leading to significant resistance to the degradation. However, the longer dipping time and heating could lead to a broken N-Si-Cellulose network and thus may not resist fire effectively. In addition, maximum degradation occurred by increasing the temperature from T_{on} to T_{off} for DI-5h-RT up to ~700 °C, which is a relatively larger temperature period

with respect to the other samples. Lowering of the T_{on} and T_{off} temperature values for the sample DI-2h-15 resulted a positive decrease in the peak degradation temperature of the respective sample. In addition, to explore the peak degradation temperature, the derivative of the TGA curves (DTGA) was obtained, as shown as Figure 5. The maximum peak degradation temperature was recorded as $\sim 367.34^\circ\text{C}$ for the sample DI-5 h-RT, while the lowest peak degradation temperature was recorded as $\sim 341.69^\circ\text{C}$ for DI-2 h-15. The highest peak degradation temperature suggests higher stability against the heat, offered by the coated materials and char formed on the surface of the cotton fabric. From the DTGA curves, it can be seen that the char serves as an oxygen and heat barrier, which restrains the thermo-oxidative degradation of the cotton fabric at higher temperatures.

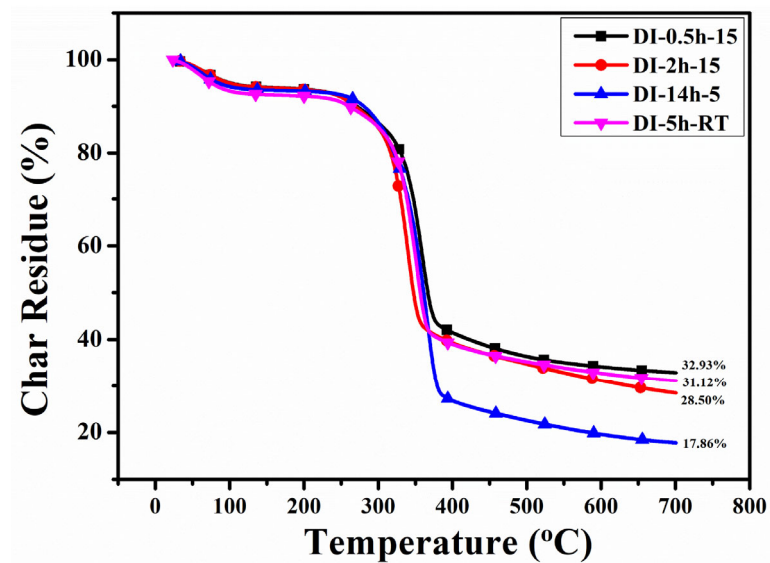


Figure 4. Thermo-gravimetric analysis curves of the coated samples.

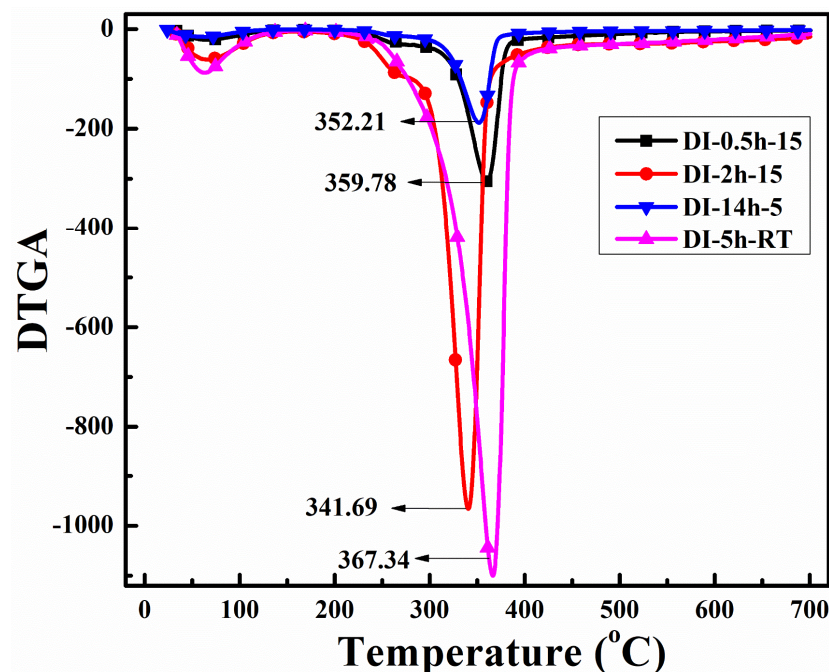


Figure 5. DTGA curves of the coated samples.

Table 3. TGA parameters of the coated fabric samples.

#	T _{on}	R _{on}	T _{off}	R _{off}	T _{peak}	Residual Char %
Uncoated						
DI-0.5 h-15	308.62	93.52	377.54	40.14	359.78	32.93
DI-2 h-15	296.53	93.82	357.90	40.30	341.69	28.50
DI-14 h-5	311.8	92.65	381.89	26.22	367.34	17.86
DI-5 h-RT	314.09	92.02	366.59	39.74	372.21	31.12

According to the VFT results, shown in Figure 6, it can be seen that the samples dipped for longer times and heat treated were mechanically rigid, damaged and broken, in addition to presenting a shift in color. Moreover, from the flame spread, as in the 10 s images, the samples with longer heat-treated times and longer dipping times were engulfed by flames in a shortest time, compared to the other samples, which resisted the flame quite efficiently. The samples obtained with shorter dipping times and no heat treatment were found with considerable char residue and zero after-glow effects. In addition, a significant decrease in the burning rate was observed for DI-0.5 h-15 and DI-5 h-RT, which could be attributed to the effective physical barrier layer formed by the silica–melamine complex network. In addition, DI-0.5 h-15 and DI-5 h-RT can be seen as mechanically stable and thus could play a role in blocking the transfer of flame from one place to another. The lower burning rate and higher burning time, shown in Figure 7, further suggest effective catalyzing of the dehydration process by the acidic samples' complexes in the initial stage, which ultimately speed up char formation and block the spread of the flame, as mentioned in Table 4 [47–49]. However, complete extinguishing of the flame could not be obtained for any samples, suggesting that there is still room for further improvement. The residues obtained for the sample with the shorter dipping time were more integrated and compact, as can be seen in the DI-5 h-RT sample, which is in agreement with the above discussion of the drastic effect of the acidic species on the substrates.

Table 4. Results of the VFT.

Samples	Burning Rate (cm ² /s)	Burning Time (s)	Self-Extinguishing
DI-0.5 h-15	4.98	36	Not
DI-2 h-15	5.55	33	Not
DI-14 h-5	6.70	32	Not
DI-5 h-RT	6.49	30	Not

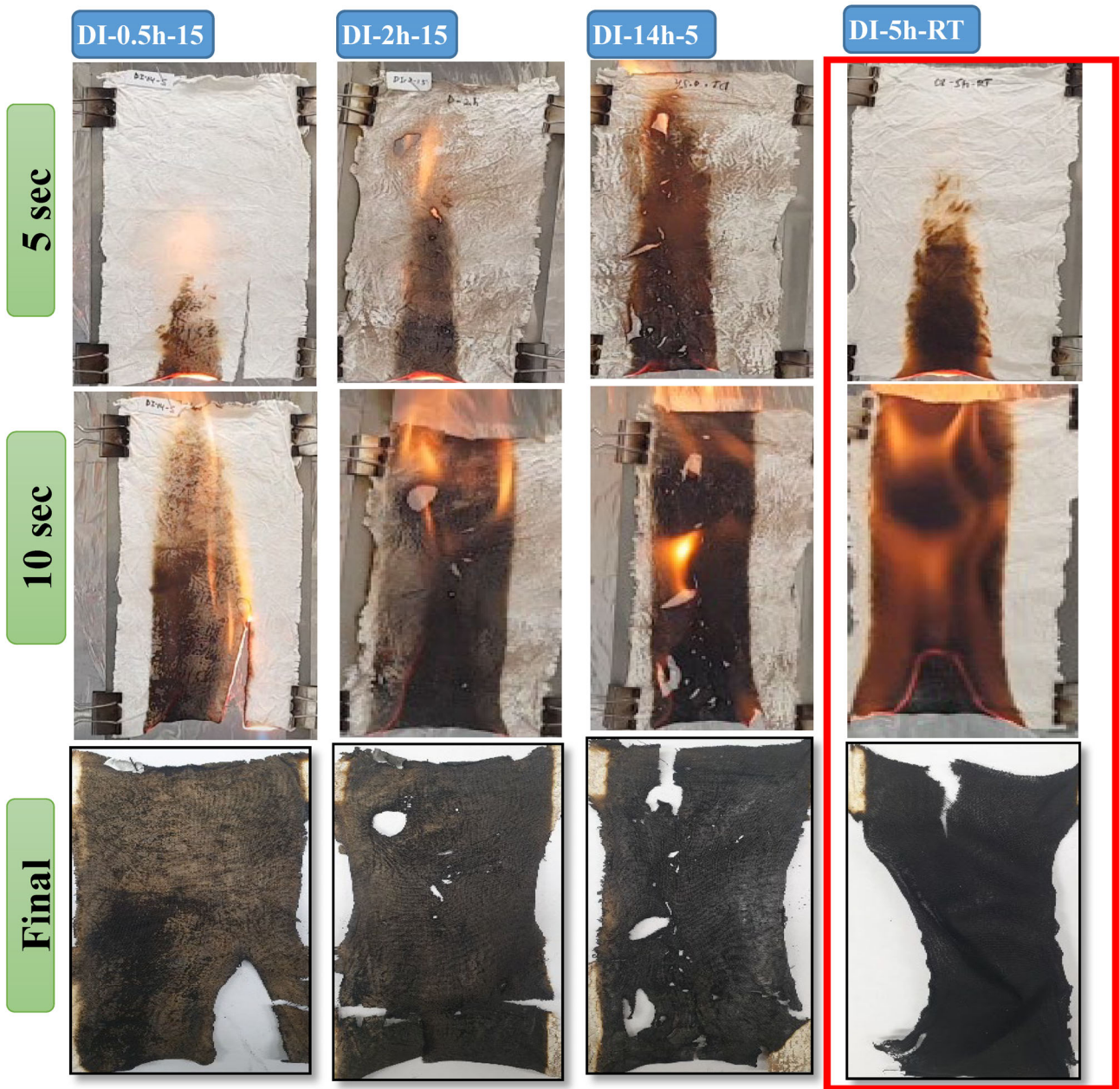


Figure 6. Images of the coated samples after burning process.

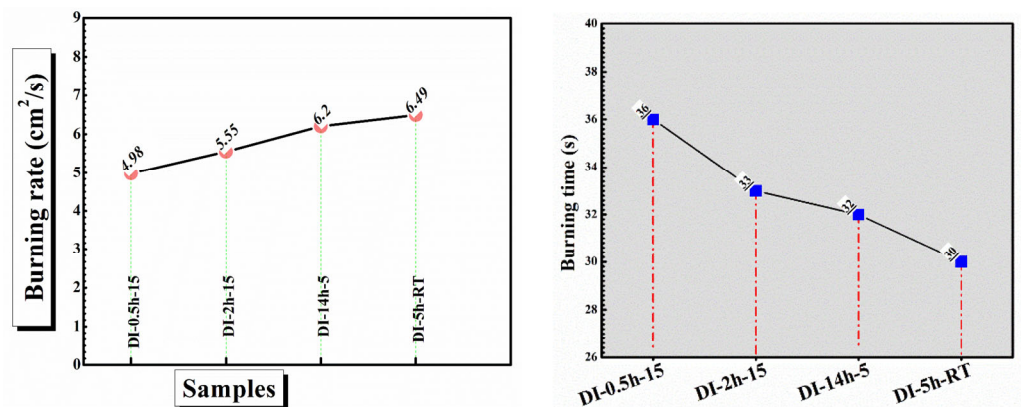


Figure 7. Burning rate and burning time obtained for the coated samples.

4. Conclusions

A Nitrogen-based (melamine)-containing sol–gel matrix was used to deposit coatings on a pure cotton fabric. The fire resistance behavior of the pure cotton fabric was greatly improved. It was found that the original color and mechanical properties of the samples with longer dipping times and a heating process of ~15 h severely impacted. In contrast, the samples obtained with shorter dipping times of 0.5 h and dried at room temperature were found to be immune to the drastic effect of the acidic samples in the sol–gel matrix. By offering effective resistance to the degradation process in the early stages, DI-0.5 h-15~32.93% produced the greatest char residue. The results were further supported by the flame spread and burning rate profile, with the lowest flame spread obtained for DI-5 h-RT.

Author Contributions: Conceptualization, Z.U.R., L.K., L.H., Y.C. and B.H.K.; methodology, Z.U.R., L.K. and B.H.K.; software, Z.U.R. and L.K.; validation, Z.U.R., L.K. and B.H.K.; formal analysis, Z.U.R., L.K. and B.H.K.; investigation, Z.U.R., L.K. and B.H.K.; resources, Z.U.R., L.K. and B.H.K.; data curation, Z.U.R., L.K., L.H., Y.C. and B.H.K.; writing—original draft preparation, Z.U.R. and L.K.; writing—review and editing, Z.U.R. and L.K.; visualization, Z.U.R., L.K., L.H., Y.C. and B.H.K.; supervision, Z.U.R., L.K. and B.H.K.; project administration, Z.U.R., L.K. and B.H.K.; funding acquisition, Z.U.R. and B.H.K. All authors have read and agreed to the published version of the manuscript.

Funding: This research was funded by the Korea National Research Foundation, grant funded by the Korean government endorsed this work (No. 2018R1A6A1A03024509 and 2021R1I1A1A01055102). This research was supported by “Regional Innovation Strategy (RIS)” through the National Research Foundation of Korea (NRF) funded by the Ministry of Education (MOE)(2021RIS-003). This work was supported by the Korea Institute of Energy Technology Evaluation and Planning (KETEP), grant funded by the Korea government (MOTIE) (20214000000480, Development of R&D engineers for combined cycle power plant technologies).

Institutional Review Board Statement: Not applicable.

Informed Consent Statement: Not applicable.

Data Availability Statement: The research data is the sole property of the university.

Conflicts of Interest: The authors declare no conflicts of interest.

References

1. Wu, Y.; Yang, Y.; Zhang, Z.; Wang, Z.; Zhao, Y.; Sun, L. Fabrication of cotton fabrics with durable antibacterial activities finishing by Ag nanoparticles. *Text. Res. J.* **2019**, *89*, 867–880. [[CrossRef](#)]
2. Cherenack, K.; van Pieterse, L. Smart textiles: Challenges and opportunities. *J. Appl. Phys.* **2012**, *112*, 091301. [[CrossRef](#)]
3. Shahidi, S.; Ghoranneviss, M. Plasma Sputtering for Fabrication of Antibacterial and Ultraviolet Protective Fabric. *Cloth. Text. Res. J.* **2016**, *34*, 37–47. [[CrossRef](#)]
4. Ashayer-Soltani, R.; Hunt, C.; Thomas, O. Fabrication of highly conductive stretchable textile with silver nanoparticles. *Text. Res. J.* **2016**, *86*, 1041–1049. [[CrossRef](#)]
5. Yetisen, A.K.; Qu, H.; Manbachi, A.; Butt, H.; Dokmeci, M.R.; Hinestroza, J.P.; Skorobogatiy, M.; Khademhosseini, A.; Yun, S.H.J.A.n. Nanotechnology in textiles. *ACS Nano* **2016**, *10*, 3042–3068. [[CrossRef](#)] [[PubMed](#)]
6. Jung, S.; Lauterbach, C.; Strasser, M.; Weber, W. Enabling technologies for disappearing electronics in smart textiles. In *Proceedings of the 2003 IEEE International Solid-State Circuits Conference*; San Francisco, CA, USA, 13 February 2003, Digest of Technical Papers; ISSCC: San Francisco, CA, USA; Volume 381, pp. 386–387.
7. Wakelyn, P.J. *Cotton Fiber Chemistry and Technology*; CRC Press: Boca Raton, FL, USA, 2007.
8. Ali, W.; Zilke, O.; Danielsiek, D.; Salma, A.; Assfour, B.; Shabani, V.; Caglar, S.; Phan, H.M.; Kamps, L.; Wallmeier, R.; et al. Flame-retardant finishing of cotton fabrics using DOPO functionalized alkoxy- and amido alkoxy silane. *Cellulose* **2023**, *30*, 2627–2652. [[CrossRef](#)]
9. Rehman, Z.U.; Huh, S.-H.; Ullah, Z.; Pan, Y.-T.; Churchill, D.G.; Koo, B.H.J.C.P. LBL generated fire retardant nanocomposites on cotton fabric using cationized starch-clay-nanoparticles matrix. *Carbohydr. Polym.* **2021**, *274*, 118626. [[CrossRef](#)]
10. Rehman, Z.U.; Kaseem, M.; Churchill, D.G.; Pan, Y.-T.; Koo, B.H.J.R.a. Macro and micro thermal investigation of nanoarchitectonics-based coatings on cotton fabric using new quaternized starch. *RSC Adv.* **2022**, *12*, 2888–2900. [[CrossRef](#)]
11. Shariatnia, Z.; Javeri, N.; Shekarriz, S. Flame retardant cotton fibers produced using novel synthesized halogen-free phosphoramidate nanoparticles. *Carbohydr. Polym.* **2015**, *118*, 183–198. [[CrossRef](#)]

12. Liang, T.; Jiang, Z.; Wang, C.; Liu, J. A facile one-step synthesis of flame-retardant coatings on cotton fabric via ultrasound irradiation. *J. Appl. Polym. Sci.* **2017**, *134*, 45114. [[CrossRef](#)]
13. Paosawatyanong, B.; Jermsutjarit, P.; Bhanthumnavin, W. Graft copolymerization coating of methacryloyloxyethyl diphenyl phosphate flame retardant onto silk surface. *Prog. Org. Coat.* **2014**, *77*, 1585–1590. [[CrossRef](#)]
14. Tsafack, M.J.; Levalois-Grützmaier, J. Towards multifunctional surfaces using the plasma-induced graft-polymerization (PIGP) process: Flame and waterproof cotton textiles. *Surf. Coat. Technol.* **2007**, *201*, 5789–5795. [[CrossRef](#)]
15. Ömeroğulları, Z.; Kut, D. Application of low-frequency oxygen plasma treatment to polyester fabric to reduce the amount of flame retardant agent. *Text. Res. J.* **2012**, *82*, 613–621. [[CrossRef](#)]
16. Pan, Y.; Zhao, H. A novel blowing agent polyelectrolyte for fabricating intumescent multilayer coating that retards fire on cotton fabric. *J. Appl. Polym. Sci.* **2018**, *135*, 46583. [[CrossRef](#)]
17. Jimenez, M.; Guin, T.; Bellayer, S.; Dupretz, R.; Bourbigot, S.; Grunlan, J.C. Microintumescent mechanism of flame-retardant water-based chitosan–ammonium polyphosphate multilayer nanocoating on cotton fabric. *J. Appl. Polym. Sci.* **2016**, *133*. [[CrossRef](#)]
18. Fang, F.; Zhang, X.; Meng, Y.; Gu, Z.; Bao, C.; Ding, X.; Li, S.; Chen, X.; Tian, X. Intumescent flame retardant coatings on cotton fabric of chitosan and ammonium polyphosphate via layer-by-layer assembly. *Surf. Coat. Technol.* **2015**, *262*, 9–14. [[CrossRef](#)]
19. Lazar, S.; Eberle, B.; Bellevergue, E.; Grunlan, J. Amine Salt Thickening of Intumescent Multilayer Flame Retardant Treatment. *Ind. Eng. Chem. Res.* **2020**, *59*, 2689–2695. [[CrossRef](#)]
20. Pan, H.; Wang, W.; Pan, Y.; Song, L.; Hu, Y.; Liew, K.M. Formation of self-extinguishing flame retardant biobased coating on cotton fabrics via Layer-by-Layer assembly of chitin derivatives. *Carbohydr. Polym.* **2015**, *115*, 516–524. [[CrossRef](#)]
21. Kundu, C.K.; Wang, X.; Hou, Y.; Hu, Y. Construction of flame retardant coating on polyamide 6.6 via UV grafting of phosphorylated chitosan and sol–gel process of organo-silane. *Carbohydr. Polym.* **2018**, *181*, 833–840. [[CrossRef](#)]
22. Kundu, C.K.; Wang, X.; Liu, L.; Song, L.; Hu, Y. Few layer deposition and sol-gel finishing of organic-inorganic compounds for improved flame retardant and hydrophilic properties of polyamide 66 textiles: A hybrid approach. *Prog. Org. Coat.* **2019**, *129*, 318–326. [[CrossRef](#)]
23. Ren, Y.; Zhang, Y.; Gu, Y.; Zeng, Q. Flame retardant polyacrylonitrile fabrics prepared by organic-inorganic hybrid silica coating via sol-gel technique. *Prog. Org. Coat.* **2017**, *112*, 225–233. [[CrossRef](#)]
24. Song, K.; Zhang, H.; Pan, Y.-T.; Ur Rehman, Z.; He, J.; Wang, D.-Y.; Yang, R. Metal-organic framework-derived bird’s nest-like capsules for phosphorous small molecules towards flame retardant polyurea composites. *J. Colloid Interface Sci.* **2023**, *643*, 489–501. [[CrossRef](#)] [[PubMed](#)]
25. Rehman, Z.U.; Pan, Y.-T.; Churchill, D.G.; Koo, B.H. Microstructural and thermal investigation of the bioinspired and synthetic fire-retardant materials deposited on cotton using LBL process. *Korean J. Chem. Eng.* **2023**, *40*, 943–951. [[CrossRef](#)]
26. Song, K.; Li, X.; Pan, Y.-T.; Hou, B.; Rehman, Z.U.; He, J.; Yang, R. The influence on flame retardant epoxy composites by a bird’s nest-like structure of Co-based isomers evolved from zeolitic imidazolate framework-67. *Polym. Degrad. Stab.* **2023**, *211*, 110318. [[CrossRef](#)]
27. Song, K.; Hou, B.; Ur Rehman, Z.; Pan, Y.-T.; He, J.; Wang, D.-Y.; Yang, R. “Sloughing” of metal-organic framework retaining nanodots via step-by-step carving and its flame-retardant effect in epoxy resin. *Chem. Eng. J.* **2022**, *448*, 137666. [[CrossRef](#)]
28. Hou, B.; Song, K.; Ur Rehman, Z.; Song, T.; Lin, T.; Zhang, W.; Pan, Y.-T.; Yang, R. Precise Control of a Yolk-Double Shell Metal–Organic Framework-Based Nanostructure Provides Enhanced Fire Safety for Epoxy Nanocomposites. *ACS Appl. Mater. Interfaces* **2022**, *14*, 14805–14816. [[CrossRef](#)]
29. Rehman, Z.U.; Niaz, A.K.; Song, J.-I.; Koo, B.H. Excellent Fire Retardant Properties of CNF/VMT Based LBL Coatings Deposited on Polypropylene and Wood-Ply. *Polymers* **2021**, *13*, 303. [[CrossRef](#)]
30. Alongi, J.; Ciobanu, M.; Tata, J.; Carosio, F.; Malucelli, G. Thermal stability and flame retardancy of polyester, cotton, and relative blend textile fabrics subjected to sol–gel treatments. *J. Appl. Polym. Sci.* **2011**, *119*, 1961–1969. [[CrossRef](#)]
31. Lin, D.; Zeng, X.; Li, H.; Lai, X.; Wu, T. One-pot fabrication of superhydrophobic and flame-retardant coatings on cotton fabrics via sol-gel reaction. *J. Colloid Interface Sci.* **2019**, *533*, 198–206. [[CrossRef](#)]
32. Zhu, Z.-M.; Xu, Y.-J.; Liao, W.; Xu, S.; Wang, Y.-Z. Highly Flame Retardant Expanded Polystyrene Foams from Phosphorus–Nitrogen–Silicon Synergistic Adhesives. *Ind. Eng. Chem. Res.* **2017**, *56*, 4649–4658. [[CrossRef](#)]
33. Wang, X.; Romero, M.Q.; Zhang, X.-Q.; Wang, R.; Wang, D.-Y. Intumescent multilayer hybrid coating for flame retardant cotton fabrics based on layer-by-layer assembly and sol–gel process. *RSC Adv.* **2015**, *5*, 10647–10655. [[CrossRef](#)]
34. Kundu, C.K.; Li, Z.; Song, L.; Hu, Y. An overview of fire retardant treatments for synthetic textiles: From traditional approaches to recent applications. *Eur. Polym. J.* **2020**, *137*, 109911. [[CrossRef](#)]
35. Alongi, J.; Ciobanu, M.; Malucelli, G. Novel flame retardant finishing systems for cotton fabrics based on phosphorus-containing compounds and silica derived from sol–gel processes. *Carbohydr. Polym.* **2011**, *85*, 599–608. [[CrossRef](#)]
36. Cheng, X.-W.; Liang, C.-X.; Guan, J.-P.; Yang, X.-H.; Tang, R.-C. Flame retardant and hydrophobic properties of novel sol-gel derived phytic acid/silica hybrid organic-inorganic coatings for silk fabric. *Appl. Surf. Sci.* **2018**, *427*, 69–80. [[CrossRef](#)]
37. Grancaric, A.M.; Colleoni, C.; Guido, E.; Botteri, L.; Rosace, G. Thermal behaviour and flame retardancy of monoethanolamine-doped sol-gel coatings of cotton fabric. *Prog. Org. Coat.* **2017**, *103*, 174–181. [[CrossRef](#)]

38. Liu, Y.; Pan, Y.-T.; Wang, X.; Acuña, P.; Zhu, P.; Wagenknecht, U.; Heinrich, G.; Zhang, X.-Q.; Wang, R.; Wang, D.-Y. Effect of phosphorus-containing inorganic–organic hybrid coating on the flammability of cotton fabrics: Synthesis, characterization and flammability. *Chem. Eng. J.* **2016**, *294*, 167–175. [[CrossRef](#)]
39. Liang, S.; Neisius, N.M.; Gaan, S. Recent developments in flame retardant polymeric coatings. *Prog. Org. Coat.* **2013**, *76*, 1642–1665. [[CrossRef](#)]
40. Guido, E.; Alongi, J.; Colleoni, C.; Di Blasio, A.; Carosio, F.; Verelst, M.; Malucelli, G.; Rosace, G. Thermal stability and flame retardancy of polyester fabrics sol–gel treated in the presence of boehmite nanoparticles. *Polym. Degrad. Stab.* **2013**, *98*, 1609–1616. [[CrossRef](#)]
41. Alongi, J.; Ciobanu, M.; Malucelli, G. Sol–gel treatments on cotton fabrics for improving thermal and flame stability: Effect of the structure of the alkoxysilane precursor. *Carbohydr. Polym.* **2012**, *87*, 627–635. [[CrossRef](#)]
42. Selvakumar, N.; Azhagurajan, A.; Natarajan, T.S.; Mohideen Abdul Khadir, M. Flame-retardant fabric systems based on electrospun polyamide/boric acid nanocomposite fibers. *J. Appl. Polym. Sci.* **2012**, *126*, 614–619. [[CrossRef](#)]
43. Jiang, Z.; Wang, C.; Fang, S.; Ji, P.; Wang, H.; Ji, C. Durable flame-retardant and antidroplet finishing of polyester fabrics with flexible polysiloxane and phytic acid through layer-by-layer assembly and sol–gel process. *J. Appl. Polym. Sci.* **2018**, *135*, 46414. [[CrossRef](#)]
44. Zhang, D.; Williams, B.L.; Shrestha, S.B.; Nasir, Z.; Becher, E.M.; Lofink, B.J.; Santos, V.H.; Patel, H.; Peng, X.; Sun, L. Flame retardant and hydrophobic coatings on cotton fabrics via sol-gel and self-assembly techniques. *J. Colloid Interface Sci.* **2017**, *505*, 892–899. [[CrossRef](#)] [[PubMed](#)]
45. Kowalczyk, D.; Brzeziński, S.; Kamińska, I. Multifunctional bioactive and improving the performance durability nanocoatings for finishing PET/CO woven fabrics by the sol–gel method. *J. Alloys Compd.* **2015**, *649*, 387–393. [[CrossRef](#)]
46. Wang, Y.; Liu, L.; Ma, L.; Yuan, J.; Wang, L.; Wang, H.; Xiao, F.; Zhu, Z. Transparent, flame retardant, mechanically strengthened and low dielectric EP composites enabled by a reactive bio-based P/N flame retardant. *Polym. Degrad. Stab.* **2022**, *204*, 110106. [[CrossRef](#)]
47. Wang, C.; Huo, S.; Ye, G.; Wang, B.; Guo, Z.; Zhang, Q.; Song, P.; Wang, H.; Liu, Z. Construction of an epoxidized, phosphorus-based poly(styrene butadiene styrene) and its application in high-performance epoxy resin. *Compos. Part B Eng.* **2024**, *268*, 111075. [[CrossRef](#)]
48. Ao, X.; Vázquez-López, A.; Mocerino, D.; González, C.; Wang, D.-Y. Flame retardancy and fire mechanical properties for natural fiber/polymer composite: A review. *Compos. Part B Eng.* **2024**, *268*, 111069. [[CrossRef](#)]
49. Yu, M.; Zhang, T.; Li, J.; Tan, J.; Zhu, X. Synthesis of a Multifunctional Phosphorus/Silicon Flame Retardant via an Industrial Feasible Technology. *ACS Sustain. Chem. Eng.* **2023**, *11*, 11965–11977. [[CrossRef](#)]

Disclaimer/Publisher’s Note: The statements, opinions and data contained in all publications are solely those of the individual author(s) and contributor(s) and not of MDPI and/or the editor(s). MDPI and/or the editor(s) disclaim responsibility for any injury to people or property resulting from any ideas, methods, instructions or products referred to in the content.